

OXAZIRIDINE (C-CH₃NO), C-CH₂NO RADICALS AND Cl, NH₂ AND METHYL DERIVATIVES OF OXAZIRIDINE; STRUCTURES AND QUANTUM CHEMICAL PARAMETERS

Mohammad Taghi Taghizadeh*, Morteza Vatanparast, Saeed Nasirianfar

University of Tabriz, Faculty of Chemistry, 29, Bahman Blvd., Tabriz 51666-14766, Iran

*e-mail: mttaghizadeh1947@gmail.com, mttaghizadeh@tabrizu.ac.ir; phone: (+98) 41 33 393 137; fax: (+98) 41 33 340 191

Abstract. Oxaziridine [c-CH₃NO (X¹A)], c-CH₂NO (X²A) radicals and Cl, NH₂ and methyl derivatives of oxaziridine structures have been optimized via DFTB3LYP level of theory using 6-311++G (d, p) basis set. Population analysis had been carried out. Vertical ionization energy (VIE) and adiabatic ionization energy (AIE), Fukui indices and some quantum chemical parameters were calculated. N-O bond was determined as weakest bond in oxaziridine triangle. The effect of electron withdrawing and electron donating groups on stability of weakest bond were assessed.

Keywords: oxaziridine, DFT, Fukui function, vertical ionization energy, adiabatic ionization energy.

Received: August 2015/ Revised final: October 2015/ Accepted: October 2015

Introduction

Oxaziridine [c-CH₃NO (X¹A)] (structure 1 in Figure 1) has a triangular heterocycle containing oxygen, nitrogen, and carbon.

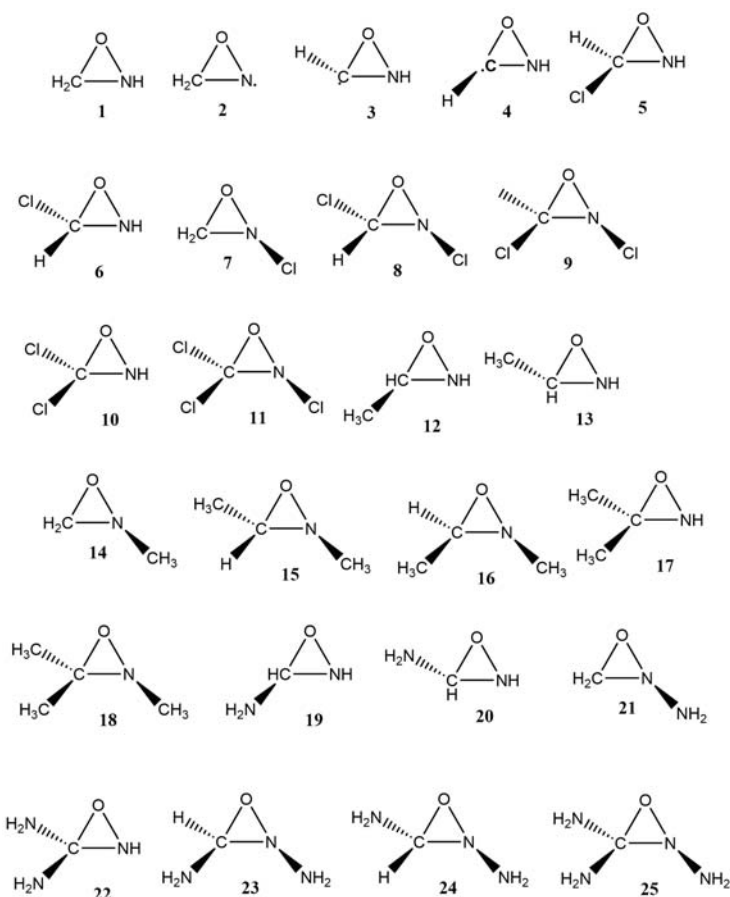


Figure 1. Structures have been investigated in this study:

(1) oxaziridine [CH₃NO (¹A)] (2) radical 1 [CH₂NO (²A)] (3) radical 2 [CH₂NO (²A)] (4) radical 3 [CH₂NO (²A)] (5) CH₂NOCl (¹A) (6) CH₂NOCl (¹A) (7) CH₂NOCl (¹A) (8) CHNOCl₂ (¹A) (9) CHNOCl₂ (¹A) (10) CHNOCl₂ (¹A) (11) CNOCl₃ (¹A) (12) C₂H₅NO (¹A) (13) C₂H₅NO (¹A) (14) C₂H₅NO (¹A) (15) C₃H₇NO (¹A) (16) C₃H₇NO (¹A) (17) C₃H₇NO (¹A) (18) C₄H₉NO (¹A) (19) CH₄N₂O (¹A) (20) CH₄N₂O (¹A) (21) CH₄N₂O (¹A) (22) CH₅N₃O (¹A) (23) CH₅N₃O (¹A) (24) CH₅N₃O (¹A) (25) CH₆N₄O (¹A).

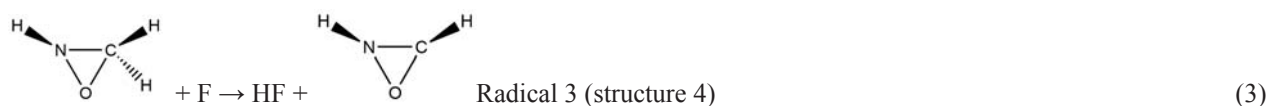
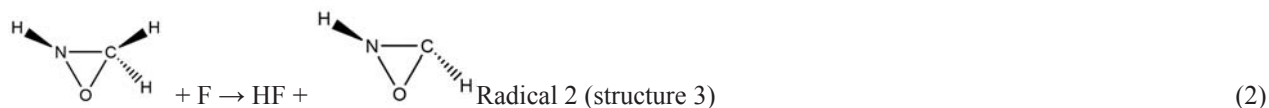
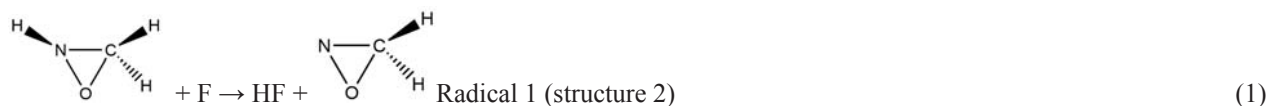
Oxaziridine derivatives were first discovered by Emmons [1]. A series of N-protected oxaziridines as electrophilic amination reagents were studied by Vidal et al. [2, 3] and Armstrong and Cooke [4]. Armstrong and Draffan researched on intramolecular epoxidation in oxaziridines [5]. Oxyfunctionalization of nonactivated sites were studied by Arnone et al. [6]. Research on synthesis and properties of 3, 3-disubstituted N-sulfonyloxaziridine [7] have been worked by Davis and et al. Also they investigated the kinetics and mechanism of the oxidation of oxaziridines [8] and their applications in organic synthesis [9].

Transition states of epoxidation and stereo selectivity in oxaziridines were investigated by Houk and et al. [10]. Oxaziridines have been studied as intermediate and their activation has been investigated [11, 12]. Oxygen and nitrogen typically act as nucleophiles due to their high electronegativity that lead to weak N-O bond. Unusual reactivity of oxaziridine is due to the highly strained three-membered ring and the relatively weak N-O bond.

Because of unstable nature of oxaziridine structure, most of studies have been implemented on oxaziridine derivatives [13] and oxaziridine as intermediate [14]. Some theoretical studies have been carried out on oxaziridine [$c\text{-CH}_3\text{NO}$ ($X^1\text{A}$)] [15, 16]. All structures have been showed in Figure 1. Optimized structures with B3LYP/6-311++G(d,p) have been represented in Figure S1 (*Supplementary material*).

Computational details

In this study oxaziridine [$c\text{-CH}_3\text{NO}$ ($X^1\text{A}$)] (structure 1) reaction with fluorine atom (F) has been presumed that produce HF and a radical [$c\text{-CH}_2\text{NO}$ ($X^2\text{A}$)], and possible reactions are presented in Eq.(1), Eq.(2) and Eq.(3). One of the oxaziridine hydrogen atoms has been removed by F atom. Three probable cyclic radical have been produced.



All geometries have been optimized by Density Functional B3LYP method with 6-311++G (d, p) basis set. Use of this basis set is ordinary for C, H, N, and O and obtained results are in good agreement with experimental ones [17].

Vertical Ionization Energy (*VIE*), Adiabatic Ionization Energy (*AIE*), global hardness (η), global softness (*S*), chemical potential (μ), electronegativity (χ) and electrophilicity (ω) have been calculated. Natural bond orbital (*NBO*) analysis has been used for study of oxaziridine and its radicals and derivatives. Changes in free energy and chemical potential for reactions (1)-(3) were calculated. It can be noted that results of calculations belong to the gas phase. Before this, MP2 and B3LYP have been used for ring opening study [18]; B3LYP has been used for study of interaction between chemical species [19] and for study of complex compounds [20]. The effect of substituted groups on bond strength in ring and vertical ionization energy has been studied. For finding weak bond in molecule and radicals, *NBO* charges, and population analysis have been used. Geometry and structure parameters have been used by Arnold and Carpenter [18] for study of ring opening in cyclopropyl radical and cyclopropyl cation.

In this study Cl has been used as electron withdrawing group, and NH_2 and CH_3 groups have been used as electron donor groups. All calculations were performed with the GAMESS program suite [21].

Results and discussion

Structures

Oxaziridine (c-CH₃NO) Molecule and c-CH₂NO radicals

Geometry of oxaziridine (structure 1) and three radicals were optimized. Optimized geometries are presented in Table S1 (*Supplementary material*) and Figure S1. Important structural parameters have been presented in Table 1. Results are in good agreement with the results of Turecek et al. [16]. Vibrational frequencies have been computed for all optimized structures to ensure that the local minima had no imaginary frequencies and the excited species had one.

C-O bond in radical 1 (structure 2) is longer than this bond in oxaziridine, but in radicals 2 (structure 3) and 3 (structure 4) this bond is smaller than molecule C-O. C-N-O angle is against C-O bond. This angle increased in radical 1 but decreased in radicals 2 and 3. This evidence shows that C-O bond is weak in radical 1 in comparison with oxaziridine molecule and radicals 2 and 3. C-N bond decreased some deal in all radicals. N-O-C angle increased a little in radical 1 and decreased a little in radicals 2 and 3. N-O bond length decreased in radical 1 and increased in radicals 2 and 3.

O-C-N angle that against N-O bond decreased in radical 1 and increased in radicals 2 and 3. In radical 1 N-O bond length is near to double bond and this bond can be viewed as N=O.

Table 1

Comparison of ring structure in compounds, calculated by B3LYP/6-311++G (d,p).

Structure	Bond lengths (Å)			Bond angles (°)		
	C-O	C-N	O-N	O \hat{C} N	C \hat{N} O	C \hat{O} N
1	1.398	1.436	1.496	63.7	56.9	59.4
2	1.426	1.429	1.383	58.0	60.9	61.1
3	1.347	1.414	1.544	68.0	54.0	58.1
4	1.348	1.409	1.541	67.9	54.1	57.9
5	1.365	1.421	1.522	66.2	55.2	58.7
6	1.369	1.424	1.513	65.6	55.5	59.0
7	1.408	1.445	1.436	60.4	58.5	61.0
8	1.377	1.439	1.468	62.8	56.5	60.7
9	1.378	1.448	1.481	63.2	56.1	60.7
10	1.350	1.419	1.530	67.0	54.3	58.6
11	1.359	1.450	1.498	64.4	54.9	60.8
12	1.403	1.438	1.499	63.7	57.0	59.3
13	1.404	1.440	1.497	63.5	57.0	59.4
14	1.405	1.425	1.499	64.0	57.4	58.7
15	1.410	1.429	1.501	63.8	57.5	58.7
16	1.409	1.433	1.502	63.8	57.3	58.9
17	1.410	1.443	1.499	63.4	57.2	59.4
18	1.417	1.439	1.501	63.4	57.6	59.0
19	1.409	1.427	1.516	64.6	57.1	58.3
20	1.386	1.450	1.516	64.6	55.7	59.8
21	1.391	1.421	1.648	71.7	53.3	55.0
22	1.402	1.442	1.522	64.7	56.4	59.0
23	1.314	1.529	2.022	90.3	40.5	49.1
24	1.369	1.437	1.768	78.1	49.3	52.7
25	1.310	1.530	2.038	91.4	40.0	48.6

H3-C-H4 angle in radicals are some larger than this angle in oxaziridine. Order of ring angles in oxaziridine is: OCN > CON > CNO. That depict O-N bond is weak.

Order of ring angles in radical 1 is: CON > CNO > OCN. The decreasing of N-O bond length in radical 1 and comparison of radical 1 ring angles with oxaziridine angles show that N-O bond in radical 1 strengthen.

Orders of ring angles in radicals 2 and 3 are: OCN > CON > CNO. Study on bond length and angles in these radicals and compare them with correspondent bonds and angles in oxaziridine show that N-O bond weaken and indeed this bond is broken and ring is opened. This result is in good agreement with other results [2-4, 15, 16, 18].

Cations structure

For calculation of adiabatic ionization energy (AIE) the geometry optimization has been carried out for cations. Optimized geometries of cations are presented in Table S1 (*Supplementary material*). Results are in good agreement with the Tureceket et al. work [16].

Oxaziridine in comparison with its positive ion:

H3-C-H4 angle in ion is larger than this angle in molecule. C-O bond and C-N-O angle increase in cation. In comparison with oxaziridine, C-N bond and C-O-N angle in ion have not important change. N-O bond in cation is shorter than this bond in oxaziridine and O-C-N angle is smaller than this angle in molecule. This evidence presents that N-O bond strengthen in cation in comparison with this bond in oxaziridine. This leads to decreasing of N-O bond cleavage probability, but C-O bond weaken.

Radical 1 in comparison with its positive ion:

H3-C-H4 in ion is larger than this angle in radical. C-O bond length and C-N-O angle in cation increase. C-N bond and C-N-O angle do not show important change in comparison with radical 1. N-O bond and N-C-O angle in cation decrease. This evidence shows that N-O bond in cation strengthen but C-O bond weaken.

Radical 2 in comparison with its positive ion:

C-O bond length and C-N-O angle in cation decrease. C-N bond length and C-N-O angle in cation decrease too. But N-O bond length and N-C-O angle in cation increase. In cation C-O and C-N bonds shortened, but N-O bond weaken and most probable bond breaking happen for N-O bond that leads to ring opening.

Radical 3 in comparison with its positive ion:

C-O bond length and C-N-O angle decrease in cation. C-N bond and C-N-O angle in cation decrease too. But N-O bond length and N-C-O angle in cation increase. C-O and C-N bonds strengthen and N-O bond weaken and breaking in cation, that leads to ring opening. In comparison with $C_3H_7^+$ with C-C bond length 1.4 Å and 1.8 Å [22]; ring bonds in oxaziridine radical cations are small.

Cl, NH₂ and methyl derivatives structures

For comparison, ring structure, C-O, C-N and N-O bond lengths and corresponding angles in oxaziridine ring were presented in Table 1. Cl acts as electron withdrawing group and NH₂ and CH₃ act as electron donating groups. In *c*-CH₂NOCl (structures 5, 6 and 7) Cl acts as electronegative atom. In these compounds C-N bond do not show important change in comparison with oxaziridine (structure 1). C-O bond strengthen in structures 5 and 6 but do not has important change in structure 7. N-O bond length in structures 5 and 6 are longer than bond length in structure 1, but decrease of this bond in structure 7 shows that N-O bond strengthen in this structure. Because of Cl electronegativity, negative charge on N atom decrease and repulsion between N and O decrease. No important changes have been seen in *c*-CHNOCl₂ (structures 8, 9 and 10) and *c*-CNOC₃ (structure 11) bond lengths and bond angles.

Also, *c*-CH₂NOCH₃ (structures 12, 13 and 14), *c*-CHNOC₂H₆ (structures 15, 16 and 17) and *c*-CNOC₃H₉ (structure 18) do not show important changes in bond lengths and bond angles.

In *c*-CH₂NONH₂ (structures 19, 20 and 21) C-O bond do not have important change, C-N bond shortened and strengthen, but N-O bond can be larger than structure 1. This means that N-O bond are weak in structures 19, 20 and 21 in comparison with structure 1. In *c*-CHNON₂H₄ (structures 22, 23 and 24) C-O bond length in 22 is near to C-O bond length in 1 but in 23 and 24 this bond length decrease and bond strengthen. C-N bond in 23 in comparison with 1 is large and weak. This bond length in 22 and 24 is near to 1 amount. N-O bond length in 22, 24 and special in 23 is longer than 1. Bond lengths and angles in structure 25 are similar to 23. In both of them NN linkage are double bond and do not exist N-O bond. This means that structures 23 and 25 do not exist. Optimum geometry of them was presented in Figure 2.

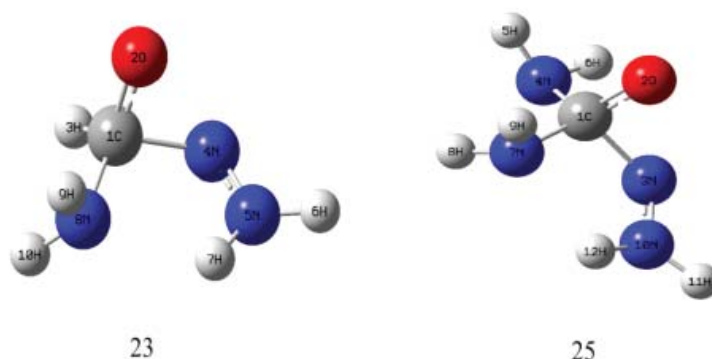


Figure 2. Optimum geometry of (23) CH₅N₃O and (25) CH₆N₄O with double bond and cleavage ring.

It should be noted that bond lengths 1.492 Å for N-O, 1.420 Å for C-O and 1.460 Å for C-N have been seen in almost stable structure (CHPhNCOOCH₃O) [2]. But 2.02 Å and 1.035 Å for N-O, 1.47 Å and 1.801 Å for C-O and 1.39 Å and 1.357 Å for C-N have been reported for transition states [10, 23]. In a work on photochemical and thermal rearrangement of oxaziridines bond lengths of N-O, C-O and C-N is 1.535 Å, 1.428 Å and 1.456 Å respectively [24]. Furthermore in theoretical study of the mechanisms of iron-catalyzed amino hydroxylation reactions, 1.48 Å, 1.41 Å and 1.46 Å have been reported for N-O, C-O and C-N bond length respectively in N-sulfonyloxaziridine [12].

Atomic charge

It is possible to note that the values of Mulliken charges on atoms are substantially different from those obtained in the NBO analysis. Along with this, it should be noted that it is difficult to judge about the orders of the corresponding bonds by the overlap population values [25].

Atomic charges are presented in Table S2 (*Supplementary material*). N, O and C atoms make ring. N and O atoms have negative charge but carbon atom has positive charge. Negative charge on O atom in three radical deal some decreases in comparison with oxaziridine. Positive charge on C atom decreases in radical 1 but increase in radicals 2 and 3. Considering charges on N atom in oxaziridine molecule and radicals depict that nitrogen charge in radical 1 decreases, but in radicals 2 and 3 increases a little.

Severe decrease of negative charge on nitrogen atom in radical 1 shows that most of this charge share with neighboring atoms and strengthen C-N and O-N bonds. Dipole moment shows the molecular charge distribution and

is given as a vector in three dimensions. It can depict the charge movement across the chemical species depends on the center of charges [26]. In oxaziridine dipole moment vector is oriented to C-H bond, in radical 1 is oriented to C atom, in radicals 2 and 3 is oriented to C-N bond. In radical 1 negative charge contributed with neighbouring atoms and dipole moment oriented to carbon. But in radicals 2 and 3, dipole moment is oriented to C-N bond. Decreasing of negative charge on O and N atoms in radical 1 (structure 2) cause the N-O bond strengthen.

Molecular electrostatic potential (*MEP*) gives many data about the electrostatic effect produced by total charge distribution of the chemical space [27]. It also depicts the relative polarity of the molecule [28]. An electronic density isosurface mapped with electrostatic potential surface show the size, shape, charge density and reactive sites of the molecules [27]. *MEP* and the electronic density are related together; it is a useful descriptor to indicate sites for electrophilic and nucleophilic reactions [29-31].

To study on reactive sites for electrophilic and nucleophilic attack the molecular electrostatic potential (*MEP*) were calculated using DFTB3LYP method and 6-311++G(d,p) basis set for optimum geometry of compounds. The negative part of *MEP* was related to electrophilic reactivity (presented by red and yellow), the positive part to nucleophilic reactivity (shown by blue) and green represents regions of zero potential [27] (Figure 3). In oxaziridine (structure 1) the negative regions are on oxygen and nitrogen atoms, at the same time the hydrogen atoms are positive. In structures 2, 3 and 4, the negative charge on O and N atoms is weaker than in structure 1, but they are obedient of structure 1 charge order. In Cl derivatives of oxaziridine (structures 5-11) the chlorine atom contribute to decreasing of negative charge on O and N in molecules and the most of negative regions are presented in green (zero potential), but hydrogen remain positive. In structure 11 chlorine atoms give some positive charge.

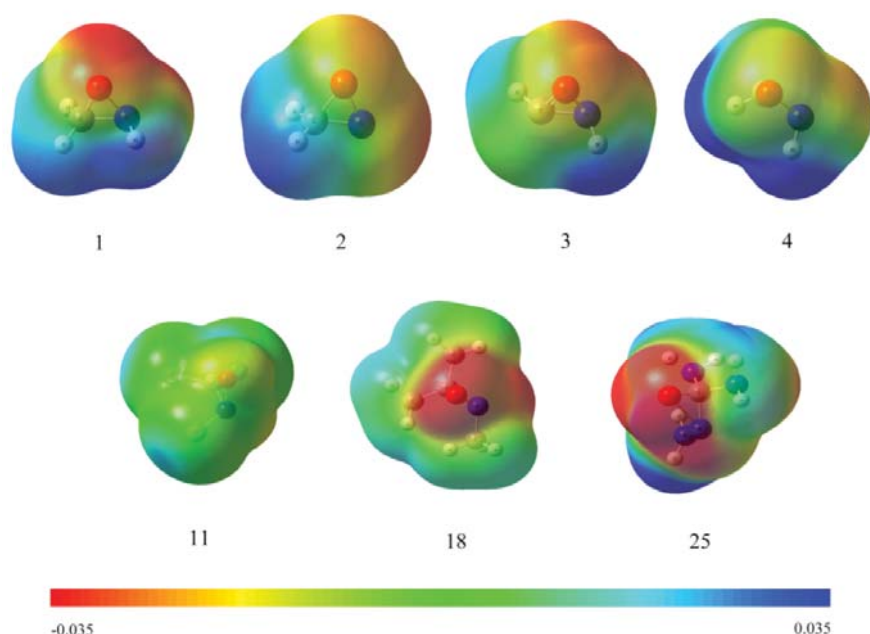


Figure 3. Molecular electrostatic potential map calculated by B3LYP/6-311++G(d,p) method. Only structures 1, 2, 3, 4, 11, 18 and 25 have been shown.

In the methyl derivatives of oxaziridine (structures 12-18), the methyl group have been amplified negative charge on O and N atoms, in comparison with Cl derivatives. In the NH_2 derivatives of oxaziridine (structures 19-25) the negative charge mostly are on oxygen atom and nitrogen atom in ring, but when the number of NH_2 groups is increasing the negative charge on the nitrogen ring is decreasing. In all cases the positive charge are on hydrogen atoms (when exist).

HOMO-LUMO

HOMO is defined as the outer occupied orbital, containing electrons that can donate electrons and *LUMO* is defined as the inner unoccupied orbital, containing free places to accept electrons. Considering *HOMO* coefficients in oxaziridine molecule and radicals depict that O and N atomic orbitals have important contribution in *HOMO*. Also in radical 1 O and N atoms are important, but in radicals 2 and 3 C and O atoms have important contribution in *HOMO*. This evidence shows that N atomic orbitals contribution decreases in radicals 2 and 3, and N-O bonds weaken.

In oxaziridine cation the most important orbitals for produce *HOMO* are O and N atomic orbitals; that show N-O bond strengthen in ion in comparison with this bond in oxaziridine. This leads to decrease probability of N-O bond cleavage, but C-O bond weaken.

In radical 1 the atomic orbitals of O and N atoms have important contribution in *HOMO*, but in its cation furthermore O and N atoms, atomic orbitals of carbon have important role in *HOMO* producing. With considering foregoing cases, N-O bond in cation strengthen but C-O bond weaken in cation. In radical 2 and its cation in optimum geometry, the most important atomic orbitals in radical 2 that make *HOMO* are C and O atomic orbitals. But in cation, O and N atomic orbitals are important. In this case C-O and C-N bonds in ion are shortened, but N-O bond is weaken and most probability for ring opening is produced by break of N-O bond. In radical 3 the atomic orbitals of O and C are important in *HOMO*, but in its cation atomic orbitals of O and N are important in *HOMO*. In this case C-O and C-N bonds strengthen and N-O bond weaken in ion and ring opening probably happen because of N-O bond breaking.

The energy gap of *HOMO* and *LUMO* shows the chemical activity of the molecule. A chemical species with a larger *HOMO-LUMO* gap have less reactivity than one having a smaller gap [32]. Large *HOMO-LUMO* energy gap means high excitation energies for many of excited states [29]. The value of the *HOMO-LUMO* energy separation are 7.14 eV, 7.02 eV, 5.44 eV and 5.42 eV for oxaziridine, radicals 1, 2 and 3, respectively, for α spin orbitals radicals and 6.63 eV, 5.63 eV and 5.76 eV for β spin orbitals in radicals 1, 2 and 3, respectively, (values from B3LYP/6-311++G (d, p)). Oxaziridine and radical 1 have large *HOMO-LUMO* energy gap in comparison with radicals 2 and 3. Oxaziridine and radical 1 are relatively stabler than radicals 2 and 3. Difference between *HOMO-LUMO* energies are presented in Table 2. More data can be finding in Table S3 (*Supplementary material*).

Isodensity plots of the frontier molecular orbitals and energy levels of the *HOMO* and *LUMO* orbitals computed by B3LYP/6-311++G (d,p) method for Oxaziridine and for radicals 1, 2 and 3 are presented in Figure 4 and Figures S2, S3 and S4 (*Supplementary material*), respectively. Energy gap for chlorinated oxaziridines in structures 5, 6 and 10 is higher than oxaziridine (structure 1) and in structures 7, 8, 9 and 11 is smaller than of structure 1.

Table 2

Difference between *HOMO* and *LUMO* energy (eV) calculated using B3LYP/6-311++G(d,p).

Structure	Spin	$ \epsilon_{HOMO} - \epsilon_{LUMO} $	Structure	$ \epsilon_{HOMO} - \epsilon_{LUMO} $
1		7.14	12	7.01
2	α	7.02	13	7.05
	β	6.63	14	6.93
3	α	5.44	15	6.81
	β	5.63	16	6.54
4	α	5.42	17	6.82
	β	5.76	18	6.40
5		7.34	19	6.53
6		7.54	20	6.42
7		5.90	21	6.58
8		6.07	22	6.54
9		5.91	23	4.12
10		7.20	24	5.49
11		5.98	25	4.04

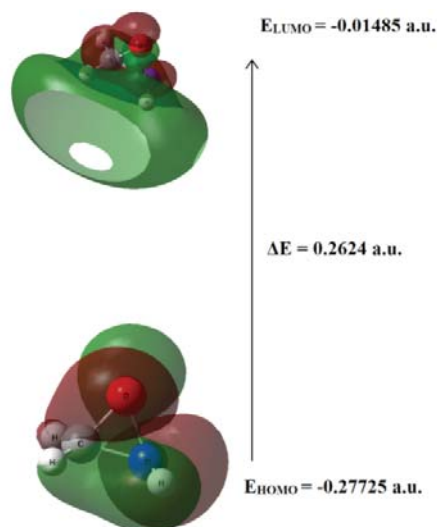


Figure 4. Isodensity plots of the frontier molecular orbitals of oxaziridine.

For methyl derivatives of oxaziridine, *HOMO-LUMO* energy gap are near and some deal smaller than structure 1 energy gap. Energy gap in NH_2 derivatives decreases in comparison with structure 1. Specially 23 and 25 structures energy gap are smaller than energy gaps in radicals 1, 2 and 3. Structures 23 and 25 have not ring and $\text{N}=\text{N}$ is a double bond (Figure 2).

NBO analysis

The *NBO* analysis have been carried out using B3LYP level of theory with 6-311++G (d,p) basis set. Selected natural bond orbital occupancies of oxaziridine and related radicals are presented in Table S4 (*Supplementary material*). Also these results for other compounds have been presented in Table S5 (*Supplementary material*). *NBO* results have been reported for both α and β spin for radicals [33, 34]. *NBO* occupancies have been used for identified π character of bonds. *NBO* occupancies show that in radical 1 N-O bond have π character and this bond strengthen in comparison with oxaziridine N-O bond, but C-O bond in radical 1 weaken, and similar to oxaziridinyl methyl radical ring opening of radical 1 by C-O bond cleavage favoured over other bonds in ring [35]. In radicals 2 and 3 C-O bond has π character and strengthened, but N-O bond weaken. This highlights the ring cleavage in radical 1 due to C-O bond breaking, but in radicals 2 and 3 because of N-O bond breaking ring opened. In other structures the bonds that make ring have single bond, except structures 23 and 25. In these structures N-O bond is broken and NN connection is double bond. Table S6 (*Supplementary material*) shows selected second order perturbation theory analysis of Fock Matrix in *NBO* Basis for structures 1-25 that calculated by B3LYP/6-311++G (d, p) method. Interaction between different parts has been studied by them.

According to this data, O2-N5 has been weaken by C1-O2 as in structures. Interactions between them in structure 2 have been weakened and leads to N-O bond strengthen. In structures 5-11 lone pair on Cl atom interacts with bonds that chlorine connect to one of the bond composer atom in ring. When methyl group connects to nitrogen on of C-H bond as donor *NBO* can affect the bonds in ring while the carbon of methyl connect to composer atom and weaken it some deal. For example in structures 14, 15, 16 and 18 C-H bond as donor impress on N-O bond in ring. Look like above, NH_2 impress on neighbouring bonds. In 23 and 25 lone pair of nitrogen atom in NH_2 -C as donor in *cis* position of $\text{N}=\text{N}$ has been weaken N-H bond in $\text{N}=\text{N}$. Furthermore, interaction between $\text{BD}^*(2)$ $\text{N}=\text{N}$ and $\text{BD}^*(1)$ $\text{N}=\text{N}$ cause the $\text{N}=\text{N}$ bond strengthen.

Quantum chemical parameters

Vertical ionization energy (*VIE*) and adiabatic ionization energy (*AIE*) were calculated for oxaziridine and three radicals. The vertical ionization energy is defined as the energy difference between the molecule in its ground state and the ion in a particular electronic state, but with the nuclei in the same positions as they had in the neutral molecule.

According to Franck-Condon principle, a vibronic transition happen so fast that nuclear positions don't change. The most intense vibrational component is said to be due to a vertical ionization, because it most closely corresponds to the vertical transition in a classical picture of the Franck-Condon principle [36]. It is to be noted that not in all cases the Franck-Condon transition is the most intensive one. The Jahn-Teller effect can bring some essential complications so that the Franck-Condon transition manifests itself as a deep well in the band shape, for example in the singlet-doublet transition [37].

Adiabatic transitions are often seen in photoelectron spectra as the first vibrational lines in the different bands [38]. *AIE* is the energy of the thermal transition between the neutral molecule in its electronic, vibrational and rotational ground state and the ion in the lowest vibrational and rotational level of a particular electronic state.

VIE has been calculated as the difference between the total energies of the neutral molecule or radical and the cation at same structure with parent molecule or radical (cation without geometry optimization). *AIE* has been computed as the total energy differences between the neutral molecule or radical and the cation at the optimum geometry.

$$VIE = E_{total}(\text{Ion in radical Z-matrix}) - E_{total}(\text{molecule or radical in optimum Z-matrix}) \quad (4)$$

$$AIE = E_{total}(\text{Ion in optimum Z-matrix}) - E_{total}(\text{molecule or radical in optimum Z-matrix}) \quad (5)$$

VIE and *AIE* of the oxaziridine and three radicals are presented in Table S7 (*Supplementary material*). Turecek et al. [16] results are in good agreement with the DFT results in this work. The difference between *VIE* and *AIE* is a crude measure of the degree of distortion of the molecule caused by ionization. The stabilization energy is equivalent to the difference between the vertical and adiabatic ionization energy for a normal band [38].

The difference between *VIE* and *AIE* is 0.92 eV, 0.64 eV, 1.45 eV and 1.50 eV for oxaziridine and radicals 1, 2 and 3, respectively. This result reveals that radical 1 cation has most likeness with parent radical (radical 1) among four structures and don't have many distortions by ionization. After radical 1 cation, cations from oxaziridine and radicals 2 and 3 have less different between cation and parent chemical species. *VIEs* have been calculated and presented in Table S8 (*Supplementary material*). In radicals 2 and 3 (structures 3 and 4) *VIE* decreases in comparison with oxaziridine and radical 1 (structures 1 and 2), because of less electronegativity in carbon atom.

In Cl substituted oxaziridines, chlorine acts as electron-withdrawing group and increases the *VIE*, but NH₂ and CH₃ act as electron donor groups that decrease the *VIE*. NH₂ is more powerful electron donor than methyl and the decreasing of *VIE* in NH₂ derivatives is more severe than of methyl derivatives (Figure 5).

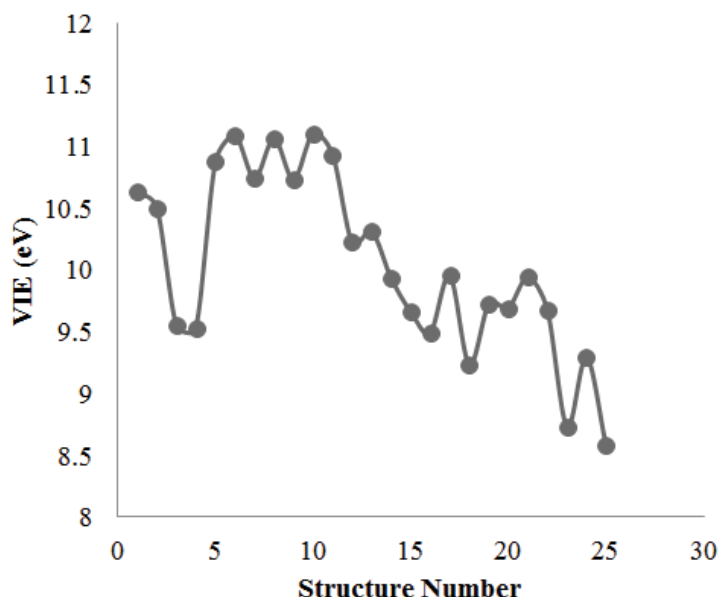


Figure 5. Effects of substituted groups (Cl, CH₃ and NH₂) on *VIE* (eV).

Furthermore, some quantum chemical parameters are calculated: ionization potential (Eq.(6)), electron affinity ((Eq.(7)), absolute electronegativity (Eq.(8)), global hardness (Eq.(9)) and global softness, *S* or σ , (Eq.(10)) [39].

$$IP = VIE \quad (6)$$

$$EA = VAE \quad (7)$$

$$\chi = \frac{IP+EA}{2} \quad (8)$$

$$\eta = \frac{IP-EA}{2} \quad (9)$$

$$S = \frac{1}{\eta} \quad (10)$$

VIE (vertical ionization energy) and *VAE* (vertical electron affinity) have been used for ionization potential and electron affinity, respectively. *VAE* was calculated as the difference between the total energies of the neutral molecule or radical and the anion at same structure with parent molecule or radical (anion without optimization geometry).

Chemical potential (Eq.(11)) is defined as the negative of the electronegativity [40]. The propensity of an electrophile to accept electrons is measured in terms of the electrophilicity within a relative scale, which is generally considered to be a kinetic quantity. Global electrophilicity index (Eq.(12)) was introduced by Parret et al. [38].

$$\mu = -\chi \text{ Or } \mu = \frac{-(IP+EA)}{2} \quad (11)$$

$$\omega = \frac{\mu^2}{2\eta} \quad (12)$$

The electrophilicity index encompasses both, the propensity of the electrophile to acquire an additional electronic charge driven and the resistance of the system to exchange electronic charge with the environment [41]. Jaque et al. [42] related the electrophilicity to electron population. The electrophilicity values follow the hardness trend.

The quantum chemical parameters of the oxaziridine and of three radicals are presented in Table S9 (*Supplementary material*).

The values of softness and hardness show that radicals 2 and 3 are softer than oxaziridine and radical 1. The changes in free energies were calculated through difference between reactants and products [43] for oxaziridine reaction with F atom (reactions 1-3). Results are presented in Table 3. Free energies were obtained from vibrational frequency calculations. These results show that reaction 1 is thermodynamically most probable than reactions 2 and 3.

Table 3

Free energy change (kJ mol⁻¹) of the reactions (1), (2) and (3), B3LYP method and 6-311++G (d, p) basis set have been used, (1Hartree = 627.5095 kcal/mol = 2625.499748 kJ/mol).

	Free energy changes
Reaction 1	-232/16
Reaction 2	-138/68
Reaction 3	-133/30

Fukui functions

Fukui functions are one of the local reactivity descriptors that explain the chemical reactivity at a particular site of chemical species [44]. Fukui indices are reactivity indices and give information about which atoms in a chemical system have a larger tendency to either lose or accept an electron that means nucleophilic or electrophilic attack, respectively. The Fukui function is defined as (Eq.(13)):

$$f(r) = \frac{\delta\rho(r)}{\delta N} r \quad (13)$$

where $\rho(r)$ is the electronic density, N is the number of electrons, r is the external potential that rooted from the nucleus.

The Fukui function indicates the preferred regions where a chemical species will change its density when the number of electrons is modified [45]. Therefore, it indicates the desire of the electronic density to deform at a certain position upon accepting or denoting electrons [46, 47]. Atomic Fukui functions on the k^{th} atom site is defined as [45]:

$$f_k^+ = q_k(N + 1) - q_k(N) \quad \text{for nucleophilic attack} \quad (14)$$

$$f_k^- = q_k(N) - q_k(N - 1) \quad \text{for electrophilic attack} \quad (15)$$

$$f_k^0 = \frac{1}{2} [q_k(N + 1) - q_k(N - 1)] \quad \text{for radical attack} \quad (16)$$

Where +, - and 0 represent nucleophilic, electrophilic and radical attack, respectively. Also q_k is the atomic charge (calculated from Mulliken population analysis) at the k^{th} atomic site is the neutral (N), anionic (N + 1) or cationic (N-1) chemical species. To calculate the Fukui function, the atomic charges have been calculated by Mulliken population analysis (MPA). Molecular geometry has been optimized by DFTB3LYP/6-311++G(d,p) method for molecule and used for MPA in molecule, cation and anion; with respect of charge and multiplicity. Fukui functions have been represented in Table 4 for oxaziridine (structure 1). This table shows negative values of the Fukui function.

Table 4

Values of the Fukui function calculated by B3LYP/6-311++G(d,p) according to Eq.(14-16).

Atom	$f_k(+)$	$f_k(-)$	$f_k(0)$
C 1	2.7895	0.0472	1.4183
O 2	-0.0852	-0.4051	-0.2451
H 3	-1.6041	-0.1270	-0.8656
H 4	-0.9829	-0.1209	-0.5519
N 5	-0.3508	-0.2786	-0.3147
H 6	-0.7664	-0.1157	-0.4411

Negative Fukui function value means that when adding an electron to the molecule, in some spots, the electron density is reduced. Alternatively, when removing an electron from the molecule, in some spots, the electron density is increased [48]. In order to solve the negative value of Fukui functions some attempts have been made by different researchers [49-51].

Kolandaivel et al. [52] introduced the atomic descriptor to characterize the local reactive sites of the chemical system. In the present study, the optimized molecular geometry has been used in single-point energy calculations, which have been performed for the anions and cations of oxaziridine (structure 1) using the ground state with doublet multiplicity. Table 4 shows the f_k^- values for the oxaziridine. It shows that C1 has higher f_k^- value in comparison with other atoms that indicates C1 is the possible site for electrophilic attack. The calculated f_k^+ value predicts that the possible site for nucleophilic attack is C1 and the radical attack was predicted at C1 site, too. By comparison of the three kinds of attacks, it has been observed that nucleophilic attack has bigger reactivity related to the radical and electrophilic attack.

Conclusions

Ab initio and DFT calculations have been performed for oxaziridine [$c\text{-CH}_3\text{NO}$ ($X^1\text{A}$)], three cyclic radicals [$c\text{-CH}_2\text{NO}$ ($X^2\text{A}$)] and Cl, NH_2 and methyl derivatives of oxaziridine. Geometries have been optimized. Bonds length and angles show that in radical 1 C-O bond weaken and in radicals 2 and 3 N-O bonds weaken, that lead to bond breaking and ring opening. Population analysis had been carried out and results confirm geometry optimization results. Some quantum chemical parameters were calculated. Radicals 2 and 3 are softer than radical 1. Free energy and chemical potential changes have been calculated for three reactions that show reaction 1 is thermodynamically most probable. All foregoing cases depict that ring opening happened because of C-O, N-O and N-O bonds cleavage in radicals 1, 2 and 3, respectively; and make cyclic radical 1 more probable than cyclic radicals 2 and 3 in oxaziridine reaction with F atom. These radicals are short life time species, among them radical 1 is more stable than radicals 2 and 3, because radicals 2 and 3 have large global softness in comparison with radical 1.

Cl atom acts as electron withdrawing group. When Cl atom conjuncts to N atom in oxaziridine ring, it forms the stable ring structure with strengthen weak bond N-O. NH_2 acts as electron donating group. Specifically, when two NH_2 groups bonded to N and C atoms in ring in *cis* position the ring structure has been destroyed, because of N-O cleavage and N=N double bond has been made. Electron withdrawing group (Cl) on N strengthen N-O bond, but Cl on C weaken N-O bond. 2 and 3 Chlorine atoms substituted on triangle don't make important change on N-O strength (in some cases weaken N-O bond a little). Electron donating groups (NH_2 and CH_3) weaken N-O bond in triangle.

In oxaziridine derivatives electron-withdrawing group (Cl) vertical ionization energy (*VIE*) increases but in electron donor groups *VIE* decreases. Calculation for Fukui functions shows that nucleophilic attack has bigger reactivity related to the radical and electrophilic attack on C1 atom.

References

- Emmons, W.D. The Preparation and properties of oxaziranes. *Journal of the American Chemical Society*, 1957, 79, pp. 5739-5754.
- Vidal, J.; Damestoy, S.; Guy, L.; Hannachi, J.C.; Aubry, A.; Collet, A. N-Alkyloxycarbonyl-3-aryloxaziridines: their preparation, structure, and utilization as electrophilic amination reagents. *Chemistry - A European Journal*, 1997, 3, pp.1691-1709.
- Vidal, J.; Hannachi, J.C.; Hourdin, G.; Mulatier, J.C.; Collet, A. N-Boc-3-trichloromethyloxaziridine: a new, powerful reagent for electrophilic amination. *Tetrahedron Letters*, 1998, 39, pp. 8845-8848.
- Armstrong, A.; Cooke, R.S. Efficient amination of sulfides with aketomalonate-derived oxaziridine: application to [2, 3]-sigmatropic rearrangements of allylic sulfimides. *Chemical Communications*, 2002, pp. 904-905.
- Armstrong, A.; Draffan, A.G. Intramolecular epoxidation in unsaturated ketones and oxaziridines. *Journal of the Chemical Society, Perkin Transactions*, 2001, 1, pp. 2861-2873.
- Arnone, A.; Foletto, S.; Metrangolo, P.; Pregnotato, M.; Resnati, G. Highly Enantiospecific Oxyfunctionalization of Nonactivated Hydrocarbon Sites by Perfluoro-*cis*-2-*n*-butyl-3-*n*-propyloxaziridine. *Organic Letters*, 1999, 1, pp. 281-284.
- Davis, F.A.; Towson, J.C.; Vashi, D.B.; Reddy, T.; McCauley, J.P.; Harakal, M.E.; Gosciniak, D.J. Chemistry of Oxaziridines. 13. Synthesis, Reactions and Properties of 3-Substituted 1, 2-Benzisothiazole 1, 1-Dioxide Oxides. *The Journal of Organic Chemistry*, 1990, 55, pp. 1254-1261.
- Davis, F.A.; Chattopadhyay, S.; Towson, J.C.; Lal, S.; Reddy, T. Chemistry of Oxaziridines. 9. Synthesis of 2-Sulfonyl- and 2-Sulfamoyloxaziridines Using Potassium Peroxymonosulfate (Oxone). *The Journal of Organic Chemistry*, 1988, 53, pp. 2087-2089.
- Davis, F.A.; Sheppard, A.C. Applications of oxaziridines in organic synthesis. *Tetrahedron*, 1989, 45, pp. 5703-5742.
- Houk, K.N.; Liu, J.; DeMello, N.C.; Condroski, K.R. Transition states of epoxidation: diradical character, spiro geometries, transition state flexibility, and the origins of stereoselectivity. *Journal of the American Chemical Society*, 1997, 119, pp. 10147-10152.

11. Srivastava, R.M.; Pereira, M.C.; Faustino, W.W. M.; Coutinho, K.; dos Anjos, J. V.; de Melo, S. J. Synthesis, mechanism of formation, and molecular orbital calculations of arylamidoximes. *Monatshefte fur Chemie*, 2009, 140, pp. 1319-1324.
12. Ren, Q.; Guan, S.; Shen, X.; Fang, J. Density Functional Theory Study of the Mechanisms of Iron Catalyzed Aminohydroxylation Reactions. *Organometallics*, 2014, 33, pp. 1423-1430.
13. Couche, E.; Fkyerat, A.; Tabacchi, R. Asymmetric Synthesis of the cis- and trans-3, 4-Dihydro-2, 4, 8-trihydroxynaphthalen-1(2H)-ones. *Helvetica Chimica Acta*, 2003, 86, pp. 210-221.
14. Seebach, D.; Yoshinari, T.; Beck, A.K.; Ebert, M.O.; Castro-Alvarez, A.; Vilarrasa, J.; Reiher, M. How small amounts of impurities are sufficient to catalyze the interconversion of carbonyl compounds and iminium ions, or is there a metathesis through 1, 3-oxazetidinium ions experiments, speculations and calculations. *Helvetica Chimica Acta*, 2014, 97, pp. 1177-1203.
15. Oliveros, E.; Riviere, M.; Malrieu, J.P.; Teichtel, C. Theoretical exploration of the photochemical rearrangement of oxaziridines. *Journal of the American Chemical Society*, 1979, 101, pp.318-322.
16. Turecek, F.; Polasek, M.; Sadilek, M. High-energy [C, H3, N, O] cation radicals and molecules. *International Journal of Mass Spectrometry*, 2000, 195-196, pp. 101-114.
17. Jankovic, N.; Bugarcic, Z.; Markovic, S. Double catalytic effect of $(\text{PhNH}_3)_2\text{CuCl}_4$ in a novel, highly efficient synthesis of 2-oxo and thioxo-1, 2, 3, 4-tetrahydropyrimidines. *Journal of the Serbian Chemical Society*, 2015, 80, pp. 595-604.
18. Arnold, P.A.; Carpenter, B.K. Computational studies on the ring openings of cyclopropyl radical and cyclopropyl cation. *Chemical Physics Letters*, 2000, 328, pp. 90-96.
19. Spataru, T.; Fernandez, F. Hydrogen molecule interaction with $\text{CpCr}(\text{Co})_3$ Catalyst. *Chemistry Journal of Moldova*, 2012, 7, pp. 21-26.
20. Gorinchoy, N.N.; Dobrova, B.; Gorbachev, M.Yu.; Munteanu, G.; Ogurtsov, I.Ya. Activation of Acetylene by Coordination to Bis-Triphenylphosphine Complex of Pt (0): DFT Study. *Chemistry Journal of Moldova*, 2009, 4, pp. 123-128.
21. Hasanzadeh, N.; Nori-Shargh, D. Correlations between hardness, electronegativity, anomeric effect associated with electron delocalizations and electrostatic interactions in 1, 4, 5, 8-tetraoxadecalin and its analogs containing S and Se atoms. *Computational and Theoretical Chemistry*, 2015, 1051, pp. 1-9.
22. Tulub, A.V.; Simon, K.V. Molecular fragmentation on collision with protons for Freon and propane molecules. *Journal of Structural Chemistry*, 2007, 48, pp. S79-S93.
23. Davis, F.A.; Chen, B.C. Asymmetric hydroxylation of enolates with N-sulfonyloxaziridines. *Chemical Reviews*, 1992, 92, pp. 919-934.
24. Lattes, A.; Oliveros, E.; RiviBre, M.; Belzecki, C.; Mostowicz, D.; Abramskj, W.; Piccinni-Leopardi, C.; Germain, G.; Van Meerssche, M. Photochemical and Thermal Rearrangement of Oxaziridines: Experimental Evidence in Support of the Stereo electronic Control Theory. *Journal of the American Chemical Society*, 1982, 104, pp. 3929-3934.
25. Sliznev, V.V.; Belova, N.V.; Girichev, G.V. An *ab initio* study of the electronic and geometric structure of bis-of dipivaloylmethane with manganese, iron, and cobalt. *Journal of Structural Chemistry*, 2010, 51, pp. 622-634.
26. Balachandran, V.; Lalitha, S.; Rajewari, S. Rotational isomers, density functional theory, vibrational spectroscopic studies, thermodynamic functions, NBO and HOMO-LUMO analyses of 2, 6-Bis (chloromethyl) pyridine. *Spectrochimica Acta, Part A*, 2012, 97, pp. 1023-1032.
27. Thul, P.; Gupta, V.P.; Ram, V.J.; Tandon, P. Structural and spectroscopic studies on 2-pyranones. *Spectrochimica Acta, Part A*, 2010, 75, pp. 251-260.
28. Balachandran, V.; Rajeswari, S.; Lalitha, S. Vibrational spectral analysis, computation of thermodynamic functions for various temperatures and NBO analysis of 2, 3, 4, 5-tetrachlorophenol using *ab initio* HF and DFT calculations. *Spectrochimica Acta, Part A*, 2013, 101, pp. 356-369.
29. Tanak, H. Quantum chemical computational studies on 2-methyl-6-[2-(trifluoromethyl) phenyliminomethyl] phenol. *THEOCHEM*, 2010, 950, pp. 5-12.
30. Luque, F.J.; Lopez, J.M.; Orozco, M. Perspective on "Electrostatic interactions of a solute with a continuum. A direct utilization of *ab initio* molecular potentials for the prevision of solvent effects". *Theoretical Chemistry Accounts*, 2000, 103, pp. 343-345.
31. Okulik, N.; Jubert, A.H. Theoretical analysis of the reactive sites of non-steroidal anti-inflammatory drugs. *Internet Electronic Journal of Molecular Design*, 2005, 4, pp. 17-30.
32. Padmaja, L.; Ravi Kumar, C.; Sajan, D.; Hubert Joe, I.; Jaya Kumar, V.S.; Pettit, G.R.; Nielsen, O.F. Density functional study on the structural conformations and intramolecular charge transfer from the vibrational spectra of the anticancer drug combretastatin-A2. *Journal of Raman Spectroscopy*, 2009, 40, pp. 419-428.
33. Sizova, O.V.; Skripnikov, L.V.; Sokolov, A.Y.; Lyubimova, O.O. Features of the electronic structure of ruthe-

- nium tetracarboxylates with axially coordinated nitric oxide (II). *Journal of Structural Chemistry*, 2007, 48, pp. 28-36.
34. de Aguiar, I.; Lima, F.C.A.; Ellena, J.; Malta, V.R.S.; Carlos, R.M. Study of the phenanthroline-Mn-imidazole bonding in Mn (I) triscarbonyl complex: A X-ray and DFT computational analysis. *Computational and Theoretical Chemistry*, 2011, 965, pp. 7-14.
 35. Pasto, D. J. Ab initio theoretical studies on the ring-opening modes of the oxiranyl-, aziridinyl-, oxaziridinyl-, and thiaranylmethyl radical systems. *Journal of Organic Chemistry*, 1996, 61, pp. 252-256.
 36. Ellis, A.M.; Feher, M.; Wright, T.G. *Electronic and Photoelectron Spectroscopy: Fundamentals and Case Studies*. Cambridge University Press: Cambridge, 2005, 286 p.
 37. Perlin, Yu. E.; Tsukerblat, B. S. Optical Bands and Polarization Dichroism of Jahn-Teller Centers, in: *Dynamical Jahn-Teller Effect in Localized Systems*. Elsevier Publications: Amsterdam, 1984, pp. 251-346.
 38. Eland, J.H.D. *Photoelectron spectroscopy: an introduction to ultraviolet photoelectron spectroscopy in the gas phase*, Butterworths, 1984, pp. 105-122.
 39. Muthu, S.; Renuga, S. Molecular orbital studies (hardness, chemical potential, electronegativity and electrophilicity), vibrational spectroscopic investigation and normal coordinate analysis of 5-{1-hydroxy-2-[(propan-2-yl)amino]ethyl}benzene-1,3-diol. *Spectrochimica Acta, Part A*, 2014, 118, pp. 683-694.
 40. Iczkowski, R.P.; Margrave, J. V. Electronegativity. *Journal of the American Chemical Society*, 1961, 83, pp. 3547-3551.
 41. Campodonico, P.R.; Aizman, A.; Contreras, R. Group electrophilicity as a model of nucleofugality in nucleophilic substitution reactions. *Chemical Physics Letters*, 2006, 422, pp. 340-344.
 42. Correa, J.V.; Jaque, P.; Olah, J.; Toro-Labbe, A.; Geerlings, P. Nucleophilicity and electrophilicity of silylenes from a molecular electrostatic potential and dual descriptor perspectives. *Chemical Physics Letters*, 2009, 470, pp. 180-186.
 43. Arsene, I. The theoretical study of some reactions with the participation of O & H and HO & 2 radicals. *Chemistry Journal of Moldova*, 2008, 3, pp. 109-113.
 44. Yang, W.; Parr, R.G. Hardness, softness, and the Fukui function in the electronic theory of metals and catalysis. *Proceedings of the National Academy of Sciences of the United States of America*, 1985, 82, pp. 6723-6726.
 45. Sheela, N.R.; Sampathkrishnan, S.; Thirumalai Kumar, M.; Muthu, S. Quantum mechanical study of the structure and spectroscopic, first order hyperpolarizability, Fukui function, NBO, normal coordinate analysis of Phenyl-N-(4-Methyl Phenyl) Nitro. *Spectrochimica Acta, Part A*, 2013, 112, pp. 62-77.
 46. Ayers, P.W.; Parr, R.G.J. Variational Principles for Describing Chemical Reactions: The Fukui Function and Chemical Hardness Revisited. *Journal of the American Chemical Society*, 2000, 122, pp. 2010-2018.
 47. Parr, R.G.; Yang, W.J. Density functional approach to the frontier-electron theory of chemical reactivity. *Journal of the American Chemical Society*, 1984, 106, pp. 4049-4050.
 48. Demircioglu, Z.; Albayrak Kastas, C.; Buyukgungor, O. The spectroscopic (FTIR, UV-vis), Fukui function, NLO, NBO, NPA and tautomerism effect analysis of (E)-2-[(2-hydroxy-6-methoxybenzylidene) amino] benzonitrile. *Spectrochimica Acta, Part A*, 2015, 139, pp.539-548.
 49. Roy, R. K.; Hirao, H.; Krishnamurthy, S.; Pal, S. Mulliken population analysis based evaluation of condensed Fukui function indices using fractional molecular charge. *Journal of Chemical Physics*, 2001, 115, pp. 2901-2907.
 50. Bultinck, P.; Carbo-Dorca, R.; Langenaekar, W. Negative Fukui functions: New insights based on electronegativity equalization. *Journal of Chemical Physics*, 2003, 118, pp. 4349-4356.
 51. Bultinck, P.; Carbo-Dorca, R.; Negative and Infinite Fukui Functions: The Role of Diagonal Dominance in the Hardness Matrix. *Journal of Mathematical Chemistry*, 2003, 34, pp. 67-74.
 52. Kolandaivel, P.; Praveen, G.; Selvarengan, P. Study of atomic and condensed atomic indices for reactive sites of molecules. *Journal of Chemical Sciences*, 2005, 117, pp. 591-598.